Punjab University
Journal of Mathematics (ISSN 1016-2526)
Vol. 44(2012) pp. 9-21

MHD ASYMMETRIC FLOW BETWEEN TWO POROUS DISKS

A. R. Wehgal
Centre for Advanced Studies in Pure and Applied Mathematics
Bahauddin Zakariya University
Multan, Pakistan
Email: raufamar@yahoo.com

Muhammad Ashraf
Centre for Advanced Studies in Pure and Applied Mathematics
Bahauddin Zakariya University
Multan, Pakistan
Email: muhammadashraf@bzu.edu.pk

Abstract. A numerical study is presented for steady incompressible viscous MHD asymmetric flow of an electrically conducting fluid between two infinite parallel stationary coaxial porous disks of different permeability in the presence of a transverse magnetic field. The main flow is superimposed by a constant injection at the surfaces of the disks. The governing non linear partial differential equations together with the boundary conditions are reduced to non linear ordinary one using Von Karman's similarity transformation. An algorithm based on finite difference discretization is used to solve the obtained boundary value problem. The results are presented in tabular and graphical forms to discuss important features of the flow. Comparisons with the previously published literature work are found to be in a good agreement in the absence of magnetic field. The present investigations show that magnetic field enhances shear stresses. The position of viscous layer changes with the permeable parameter.

AMS (MOS) Subject Classification Codes: 76D05, 76W05, 65L12
Key Words: MHD flow, porous disks, asymmetric flow, similarity transformation, finite differences.

1. INTRODUCTION

The phenomenon of fluid motion between parallel disks has been of considerable interest due to its diversity of significant applications in the fields of hydrodynamical machines and apparatus, magnetic storage devices (disk drives), semiconductor manufacturing processes with rotating wafers, gas turbine engines, and other rotating machinery, viscometry, heat and mass exchanges, computer storage devices, lubrication, crystal growth processes, geothermal, geophysical, oceanography, biomechanics and in the design of thrust bearings, and radial diffusers etc. Magnetohydrodynamics (MHD) flow has

important applications in MHD pumps, aerodynamics heating, MHD power generators, accelerators, purification of crude oil, petroleum industries and polymer technology.

Siddique *et. al* [1] presented a new exact solution for MHD transient rotation flow of a second grade fluid in a porous space. Khan *et. al* [2] discussed MHD flows of a second grade fluid between two side walls perpendicular to a plate through a porous medium. Hayat *et. al* [3] studied analytically the effects of radiation on MHD flow of a Maxwell fluid in a channel with porous medium. Some exact solutions for the helical flow of a generalized Oldroyd-B fluid in a circular cylinder were presented by Fetecau *et. al* [4]. Ashraf *et. al* [5] solved numerically the problem of MHD stagnation point flow of a micropolar fluid towards a heated surface. Rudraiah and Chandrasekhara [6] considered the problem of MHD flow between parallel porous disks for large suction Reynolds number using perturbation technique. Rasmussen [7] investigated numerically the problem of steady viscous symmetric flow between two infinite parallel porous coaxial disks with uniform injection/ suction. The theorem of existence and uniqueness for non rotational fluid motion between two infinite coaxial and permeable disks was proved by Elcrat [8]. The flow between two porous coaxial disks of different permeability with heat and mass transfer was analyzed by Guar and Chaudhary [9]. An exact solution for the problem of steady viscous flow between two parallel disks was given by Phan-Thien and Bush [10]. The fluid motion was generated due to different injection/ suction velocities through the surfaces of the porous disks. Asymmetric flow between parallel rotating disks was considered by Rajagopal *et. al* [11] and numerical results were presented for the rotation about a common axis and the rotation about two distinct axes for a set of values of the governing parameters. Rajagopal *et. al* [12]] investigated asymmetric flow above a rotating disk to obtain the solutions that correspond to the flow induced by the rotation of a disk moving with a constant uniform velocity. Experimental and numerical methods were presented by Singh *et.al* [13] to study the effect of acceleration on flow field. Attia [14] studied the problem of steady incompressible viscous flow and heat transfer of an electrically conducting fluid due to the rotation of an infinite non conducting porous disk in the presence of a uniform external magnetic field by considering the ion slip. The fluid motion was subjected due to the uniform injection/ suction at the two disks. The transformed non linear differential equations together with the boundary conditions were solved numerically using the finite difference discretization. Ersoy [15] analyzed linearly viscous fluid flow between two disks rotating about two distinct vertical axes. An approximate analytical solution was given to present the dependence of velocity components on the position, the Reynolds number, the eccentricity, and the ratio of angular speeds of the disks. An exact solution for the problem of steady incompressible axisymmetric flow between two stretchable infinite disks in the absence of the body force was analyzed by Fang and Zhang [16] using an extension of Von Karman's similarity transformation to discuss the effects of disk stretching and stretching Reynolds number. The squeezed film flow between two rotating permeable disks was investigated by Bhatt and Hamza [17] using a suitable similarity solution.

Our main goal here is to address a comprehensive parametric study of flow of an asymmetric steady incompressible viscous electrically conducting fluid between two stationary coaxial infinite parallel porous disks of different permeability in the presence of uniform magnetic field which was not considered by previous authors. By using a finite difference scheme, a numerical solution is obtained for the governing momentum equation.

2. PROBLEM FORMULATION

We make use of the cylindrical polar co ordinate system $(r,\ \theta,\ z)$ for the physical problem under consideration. This study considers the case of an asymmetric steady laminar incompressible viscous flow of an electrically conducting fluid confined between two large stationary porous disks of infinite radii coinciding with the planes $z = \pm a$ with constant injection velocities V_1 and V_2 at the lower and upper disks respectively in the presence of a uniform transverse magnetic field of intensity B_0 as shown in Fig. 1.
In order to examine the effects of different permeability of the disks, we define the following permeability parameter:

$$A = 1 - \frac{V_1}{V_2}, \tag{2. 1}$$

Following works of Hayat and Wang [18] the governing equations for steady viscous flow of an electrically conducting fluid in the presence of a uniform stationary magnetic field can be written as:

$$\frac{\partial \rho}{\partial t} + \nabla \cdot (\rho \underline{V}) = 0, \tag{2. 2}$$

$$\frac{\partial \underline{V}}{\partial t} + (\underline{V} \cdot \nabla)\, \underline{V} = \underline{f} - \frac{1}{\rho}\nabla p + \upsilon\, \nabla^2 \underline{V}, \tag{2. 3}$$

$$\nabla \cdot \underline{B} = 0, \tag{2. 4}$$

$$\nabla \times \underline{B} = \mu_m \underline{J}, \tag{2. 5}$$

$$\nabla \times \underline{E} = 0, \tag{2. 6}$$

$$\underline{J} = \sigma_e(\underline{E} + \underline{V} \times \underline{B}), \tag{2. 7}$$

where ρ is the density, ∇ the gradient, $\underline{V}$ the fluid velocity vector, υ kinematic viscosity, p the pressure, $\underline{J}$ the current density, $\underline{B}$ the total magnetic field so that $\underline{B} = \underline{B}_0 + \underline{b}$, $\underline{b}$ the induced magnetic field, μ_m the magnetic permeability, $\underline{E}$ the electric field, σ_e the electrical conductivity of the fluid and dot signifies the material derivative. Moreover $\nabla \cdot \underline{J} = 0$ is obtained from Eqs. (2. 4) and (2. 5).

The uniform stationary magnetic field $\underline{B}$ is in the transverse direction and the magnetic Reynolds number is taken small [19]. As a consequence the induced magnetic field $\underline{b}$ is neglected. We further assume that there is no electric field (i.e.$\underline{E} = 0$) because there is no applied polarization voltage. This means that no energy is extracted or added to the fluid system. By employing the above flow assumptions, the electromagnetic body force occurring in Eq. (2. 3) takes the following lineralized form [20]:

$$\underline{f} = \underline{J} \times \underline{B} = \sigma_e[(\underline{V} \times \underline{B}_0) \times \underline{B}_0] = (-\sigma_e B_0^2 u, 0, 0). \tag{2. 8}$$

The components of velocity $(u,\ v,\ w)$ along radial, transverse, and axial directions for the present problem can be written as:

$$u = u(r, z),\ v = 0,\ w = w(r, z). \tag{2. 9}$$

In view of Eqs. (2. 4)-(2. 8), the governing Eqs. (2. 2)-(2. 3) for an electrically conducting incompressible fluid in the presence of a uniform magnetic field are given in dimensionless form as:

$$\frac{\partial u}{\partial r} + \frac{u}{r} + \frac{1}{a}\frac{\partial w}{\partial \eta} = 0, \tag{2. 10}$$

$$\rho(u\frac{\partial u}{\partial r} + \frac{w}{a}\frac{\partial u}{\partial \eta}) = -\frac{\partial p}{\partial r} + \mu(\frac{\partial^2 u}{\partial r^2} + \frac{1}{r}\frac{\partial u}{\partial r} - \frac{u}{r^2} + \frac{1}{a^2}\frac{\partial^2 u}{\partial \eta^2}) - \sigma_e B_0^2 u, \tag{2. 11}$$

$$\rho(u\frac{\partial w}{\partial r} + \frac{w}{a}\frac{\partial w}{\partial \eta}) = -\frac{1}{a}\frac{\partial p}{\partial \eta} + \mu(\frac{\partial^2 w}{\partial r^2} + \frac{1}{r}\frac{\partial w}{\partial r} + \frac{1}{a^2}\frac{\partial^2 w}{\partial \eta^2}), \tag{2. 12}$$

where $\eta = \frac{z}{a}$ is a similarity variable.

The boundary conditions at the two porous disks for the velocity field are specified as follows:

$$\left.\begin{array}{ll} u(r,-1)=0, & u(r,+1)=0, \\ w(r,-1)=V_1, & w(r,+1)=V_2. \end{array}\right] \tag{2. 13}$$

Where V_1 and V_2 are uniform injection velocities at the lower and upper disks respectively.

A similarity transformation similar to those of Von Karman [21] and Elkouh [22] can be used to reduce partial differential equations (2. 10)-(2. 12) into ordinary differential equations as follows:

$$\psi(r,\eta) = \frac{V_2 r^2}{2} f(\eta), \tag{2. 14}$$

$$u = \frac{1}{ra}\frac{\partial \psi}{\partial \eta} = \frac{V_2 r}{2a} f'(\eta), \tag{2. 15}$$

$$w = -\frac{1}{r}\frac{\partial \psi}{\partial r} = -V_2 f(\eta). \tag{2. 16}$$

The velocity components given in Eqs. (2. 15)-(2. 16) are compatible with the continuity Eq. (2. 10) and hence represent a possible fluid motion. Eqs. (2. 11)-(2. 12) in view of above similarity transformations (2. 15)-(2. 16) are reduced after eliminating the pressure term, as follows:

$$f^{(iv)} + R(ff''' - M^2 f'') = 0, \tag{2. 17}$$

where $R = \dfrac{\rho V_2 a}{\mu}$ is the Reynolds number and $M = \sqrt{\dfrac{\sigma_e a B_0^2}{\rho V_2}}$ is the Hartmann number. Integrating Eq. (2. 17) w.r.t η, we get

$$f''' + R(ff'' - \frac{f'^2}{2} - M^2 f') = k, \tag{2. 18}$$

where k is a constant of integration.

The boundary conditions (2. 13) in dimensionless form can be written as:

$$\left.\begin{array}{ll} f(-1) = 1 - A, & f(1) = 1, \\ f'(-1) = 0, & f'(1) = 0. \end{array}\right] \tag{2. 19}$$

The shear stress on the disks is defined as:

$$\tau_\omega = -\mu(\frac{\partial u}{\partial z})|_{z=\pm a} = -\mu \frac{r V_2}{2a^2} f''(\pm 1). \tag{2. 20}$$

We have to solve Eq. (2. 18) subject to the boundary conditions (2. 19).

3. NUMERICAL SOLUTION

The governing ordinary differential Eq. (2. 18) is highly non linear and we use a finite difference based algorithm scheme to seek its numerical solution subject to the associated boundary conditions (2. 19). Following Chamkha and Issa [23] and Ashraf *et.al* [24, 25] the order of Eq. (2. 18) can be reduced by one with the help of substitution $q = f'$. Now we have to solve the boundary value problem consisting of the folowing equations:

$$q = f' = \frac{df}{d\eta}, \tag{3. 1}$$

$$q'' + R(fq' - \frac{q^2}{2} - M^2 q) = k. \tag{3. 2}$$

subjected to the boundary conditions:

$$\left.\begin{array}{ll} f(-1) = 1 - A, & f(1) = 1 \\ q(-1) = 0, & q(1) = 0. \end{array}\right] \tag{3. 3}$$

For the numerical solution of the above boundary value problem we discretize the domain [-1, 1] uniformly with step h. Simpson's rule Gerald [26] with the formula given in Milne [27] is applied to integrate Eq. (3. 1). The central difference approximations are used to discretize Eq. (3. 2) at a typical grid point $\eta = \eta_n$ of the interval [-1, 1]. The resulting finite difference equation is given by:

$$(R\frac{h^2}{2}q_n + 2 + RM^2h^2)q_n + kh^2 = (1 + \frac{h}{2}Rf_n)q_{n+1} + (1 - \frac{h}{2}Rf_n)q_{n-1}, \tag{3. 4}$$

where h represents the grid length, $q_n \approx q(\eta_n)$ and $f_n \approx f(\eta_n)$.

The above algebraic Eq. (3. 4) is solved iteratively by using SOR method, Hildebrand [28] subject to the appropriate boundary conditions (3. 3). In order to accelerate the iterative procedure, to improve the accuracy of the solution and to have an estimate of local as well as global discretization errors, we use the solution procedure which is mainly based on the algorithm described in Syed *et. al* [29]. The iterative procedure is stopped if the following criterion is satisfied for four consecutive iterations:

$$Max(\left\|q^{(i+1)} - q^{(i)}\right\|_2, \left\|f^{(i+1)} - f^{(i)}\right\|_2) < TOL_{iter}\,, \tag{3. 5}$$

where TOL_{iter} prescribed the error tolerance. Here we have taken error tolerance at least 10^{-12} for our numerical calculations. The constant of integration k is determined by hit and trial requiring that the computed value of f at the upper boundary matches with the given boundary value of f up to at least four decimal places.

4. RESULTS AND DISCUSSION

The objective of the present work was to examine numerically the flow characteristics associated with the asymmetric steady laminar incompressible viscous flow of an electrically conducting fluid between two stationary coaxial parallel porous infinite disks in the presence of a uniform stationary magnetic field. Special attention is given to this section for the presentation of our findings in tabular and graphical forms together with the discussion and their interpretations. The numerical results for the velocity field and the shear stresses at the two disks are obtained for a range of values of the permeability parameter A, the Reynolds number R and the Hartmann number M. To obtain the accuracy of the solutions, the results are computed for three grid sizes $h = 0.02, 0.01, 0.005$ and then extrapolated on the finer grid using Richardson's extrapolation [30]. In order to establish the validity of our numerical scheme, a comparison of numerical values of axial velocity is given in Table 1. Excellent comparisons validate our numerical computations. Other source of validity of our numerical results is Fig.2 in which the present results for radial velocity for $R = -0.5$ & $M = 0.4$ are compared with the published literature results given by Elkouh [22]**.** The comparisons are found to be in a good agreement. The value of the constant of integration k taken for each set of values of the parameters $A, R\&M$ considered in the present work is given in Tables 2-4 against the corresponding case.

In order to understand the effect of the permeability parameter A and the Reynolds number R on the flow fields, it can be first noted that A is determined by the ratio of the injection velocities at the surfaces of the two porous disks whereas R is based on the injection velocity at the upper disk. The case $R = 0$, corresponds the problem of the flow with impermeable disks. In this situation A will be arbitrary and has no effect on the flow

in view of the relation V_1= (1- A)V_2 (by definition of A given in Eq. (2. 1)), where V_1= 0 =V_2. In the case when the magnitude of R is increased for a fixed value of A, it predicts the situation in which the injection velocities at the upper and lower disks are increased keeping their ratio constant. On the other hand if A is increased from 1 to 2 and R is fixed, it represents the situation in which, for a given injection velocity at the upper disk, the injection velocity at the lower disk is increased from zero to the magnitude of that at the upper disk. For $R < 0$, the case $A = 1$ corresponds to the problem of flow in which the lower disk is impermeable and the upper disk is permeable, $1 < A < 2$ corresponds to the non zero and unequal injection velocities at the lower and upper disks and $A = 2$ represents the problem of flow symmetrically driven by equal injection velocities at both the disks.

Table 2 reveals the influence of permeability parameter A on shear stresses at the disks for fixed values of R &M. It is concluded that an increase in the permeability parameter A, leads to a reduction in shear stress at the lower disk while at the upper disk the magnitude of the shear stress increases from its minimum value to its maximum value. It can be seen from Table 2 that for the case $A = 2$, the shear stresses become equal at the upper and lower disks reflecting the symmetry of the problem. Table 3 illustrates the effect of Reynolds number R on the shear stresses at the disks for $A = 1.4 \,\&\, M = 1.2$. With an increase in the injection parameter R, the shear stress at the lower disk increases and on the other hand a decrease in the magnitude of the shear stress is noted at the upper disk. It is observed that for $R = 0$, the shear stresses are same at the disks and thus showing the symmetry of the problem. The influence of the Hartmann number M is tabulated in Table 4, for a fixed value of A &R. From Table 4 we note that the Hartmann number M enhances the shear stresses at the boundaries of the disks.

The predictions based on flow behaviors between the porous disks are presented graphically for different parameters in Figs. 3-8. Figs. 3-4 show the velocity profiles for $R = -10$ & $M = 0.8$ with different values of the permeability parameter A. The velocity profiles in the axial direction under different permeability parameter illustrated in Fig. 3 are helpful in finding the position of viscous layer which is developed due to the injection at the two disks. It is noted that by increasing the values of A, the position of the viscous layer approaches towards the central plane $z = 0$. The axial velocity profiles are lower for increasing values of A. Fig. 4 depicts the velocity profiles along the radial directions for various values of A. It is observed that the radial velocity profiles rise as we increase the values of A and the velocity profile becomes symmetric for the case $A = 2$ where it attains the maximum value.

Fig. 5 plots the influence of Reynolds number R on the axial velocity profiles for typical values of A &M. It is apparent from Fig. 5 that the axial velocity takes its dimensionless value -1 at the lower disk and 1 at the upper disk with a point of inflection near the central plane $z = 0$ where the concavity is changed. It is seen that by increasing the magnitude of R from 0 to 40, the velocity profiles increase significantly. Due to the restrictions of axial velocity being -1 at the lower disk and 1 at the upper disk, a slight increase in the axial velocity profiles is observed as the magnitude of R is increased i-e$R \to -\infty$. Fig. 6 presents the effect of R on the radial velocity profile. The radial velocity profile is symmetric for $R = 0$ with respect to the central plane $z = 0$ and has the point of maximum velocity at $R = 0$. These profiles become asymmetric and shift towards the lower disk due to the inflow velocity V_2 at the upper disk. It is seen that for increasing values of R the profiles decrease near the upper disk and increase near the lower disk.

The behavior of the Hartmann number M for fixed values of A & R is shown graphically in Figs. 7-8. Fig. 7 presents an interesting effect of M on the axial velocity. The

profiles fall at the upper disk whereas a small increase near the lower disk is observed by increasing the values of M. The radial velocity profiles shift towards the lower disk and the point of maximum velocity decreases as M is increased. Furthermore it is also noted that these profiles move away from the disks but a significant change is seen at the upper disk as shown in Fig. 8.

5. CONCLUSIONS

In the present work numerical solution of the problem of MHD asymmetric flow of an electrically conducting fluid between two infinite parallel porous disks is investigated using a suitable similarity transformation. Following conclusions can be made:

(1) Shear stresses are reduced at the lower disk and are increased at the upper disk by increasing permeability A whereas an opposite trend can be noted in case of Reynolds number R.
(2) The magnetic field causes an increase in values of shear stresses on the boundaries (disks).
(3) The position of viscous layer developed due to large injection moves towards the central plane $z = 0$ as we increase A.

Acknowledgment

The authors wish to express their sincere thanks to the honorable referees for their valuable comments to improve the quality of the paper.

REFERENCES

[1] Siddique, M. Imran and D. Vieru, *A new exact solution for MHD transient rotation flow of a second grade Fluid in a Porous space*, Bulletin of the Polytechnic Institute from placeCityIasi placecountry-regionROMANIA 54 (58)**,** (2008) 27-36.

[2] M. Khan, S. Hyder Ali, T. Hayat and C. Fetecau, *MHD flows of a second grade fluid between two side walls perpendicular to plate through a porous medium*, International Journal of Non-Linear Mechanics 43, (2008) 302 – 319.

[3] T. Hayat, R. Sajjad, Z. Abbas, M. Sajid and Awatif A. Hendi, *Radiation effects on MHD flow of Maxwell fluid in a channel with porous medium*, International Journal of Heat and Mass Transfer 54, (2011) 854–862.

[4] C. Fetecau, A. Mahmood, Corina Fetecau and D. Vieru, *Some exact solutions for the helical flow of a generalized Oldroyd-B fluid in circular cylinder*, Computers & Mathematics with Applications 56, (2008) 3096-3108.

[5] M. Ashraf and M. M. Ashraf, *MHD stagnation point flow of a micropolar fluid towards a heated surface:* Applied Mathematics and Mechanics (English Edition) 32(1), (2011) 45-54.

[6] N**.** Rudraiah and B. C. Chandrasekhara, *Flow of a conducting fluid between porous disks for large suction Reynolds number*,Phys Soc. Japan 27**,** (1969) 1041-1045.

[7] H. Rasmussen, *Steady viscous flow between two porous disks*, Z. Angewn. Math. Phys. 21**,** (1970) 187-195.

[8] A. R. Elcrat, *On the radial flow of a viscous fluid between two porous disks*, Arch. Rat. Mech. Anal. 61**,** (1976) 91-96.

[9] Y. N. Guar, R. C. Chaudhary, *Heat transfer for laminar flow through parallel porous disks of different permeability* placePlaceNameIndian PlaceTypeAcademy of Sciences, section A 87A**,** (1978) 209-217.

[10] N. Phan-Thien and M. B. Bush, *On the steady flow of a Newtonian fluid between two parallel disks*, ZAMP. 35**,** (1984) 912-919.

[11] C. Y. Lai, K. R. Rajagopal, A. Z. Szeri, *Asymmetric flow between parallel rotating disks*, J. Fluid. Mech. 146, (1984) 203-225.

[12] C. Y. Lai, K. R. Rajagopal, A. Z. Szeri, *Asymmetric flow above a rotating disk*, J. Fluid. Mech. 157**,** (1985) 471-492.

[13] A. Singh, B. D. Vyas and U. S. Powel, *Investigations on inward flow between two stationary parallel disks*, Int. J. Heat and Fluid Flow 20**,** (1999) 395-401.

[14] H. A. Attia, *On the effectiveness of the ion slip on the steady flow of a conducting fluid due to a porous rotating disk with heat transder*, Tamkang J. Sci. placecountry-regionEng. 9(3)**,** (2006) 185-193.

[15] H. V. Ersoy, *An approximate solution for flow between two disks rotating in about Distinct axes at different speeds*, Hindawi Publishing Corporation Math Problems placecountry-regionEng. 2007**,** 1-16 (2007).
[16] T. Fang, Flow over a stretchable disk, Int. Com. Heat and mass transfer 35**,** (2008) 892-895.
[17] B. S. Bhatt and E. A. Hamza, *Similarity solution for the squeezed flow film between two rotating naturally permeable discs*, ZAMM. 76**,** (1996) 291-299.
[18] T. Hayat and Yongqi Wang, *Magnetohydrodynamic flow due to noncoaxial rotations of a porous disk and a fourth-grade fluid infinity,* Math Problems Eng. 2**,** (2003) 47-64.
[19] J. A. Shereliff: *A text book of magnetohydrodynamics*, Pergoman Press, placeCityOxford, 1965.
[20] V. J. Rossow, *On flow of electrically conducting fluids over a flat plate in the presence of a transverse magnetic field*, Tech Report 1358 NASA 1958.
[21] M. Von Karman, *Under laminare and turbulente*, Reibung Z. Zngew Math. Mech.1, (1921) 233-235.
[22] A. F. Elkouh, *Laminar flow between porous disks*, J. Eng. Mech. Div. ASCE. 93**,** (1967) 5375-5377.
[23] A. J Chamkha, Camille Issa, *Effects of heat generation/ absorption and thermophoresis on hydromagnetic flow with heat and mass transfer over a flat surface*, Int J Numer Methods Heat Fluid Flow 10, (2000) 432-449.
[24] M. Ashraf, M. Anwar Kamal, K. S. Syed, *Numerical simulation of a micropolar fluid between a porous disk and a non-porous disk*, Appl. Math. Modell. 33, (2009) 1933-1943.
[25] M. Ashraf, M. Anwar Kamal, K. S. Syed, *Numerical study of asymmetric laminar flow of micropolar fluids in a porous channel*, Computers and Fluids 38 (2009), 1895-1902.
[26] C. F. Gerald, *Applied numerical analysis,* Addison- Wesley Publishing Company placeCityReading StateMassachusetts (1974).
[27] W. E. Milne: *Numerical solutions of different equations*, John Willey and Sons Inc, placeStateNew York 1953.
[28] F. B. Hildebrand: *Introduction to numerical analysis*, Tata McGraw Hill Publishing Company, Ltd. 1978.
[29] K. S. Syed, G. E. Tupholme , A. S. Wood, *Iterative solution of fluid flow in finned tubes*, Taylor C and Cross J T (Eds) Proceedings of the 10^{th} international conference on numerical methods in laminar and turbulent flow, pineridge press, UK pp. 429-440 21-25 (1997).
[30] P. Deuflhard, *Order and step size control in extrapolation methods*, Numerische Mathematik 41, (1983) 399-422.

Nomenclature

A	permeability parameter
B_0	magnetic field intensity
$\underline{b}$	induced magnetic field
$\underline{E}$	electric field
h	grid size
$\underline{J}$	current density
k	constant of integration
M	Hartmann number
R	Reynolds number
TOL_{iter}	prescribed error tolerance
V_1, V_2	injection velocities at the lower and upper disks respectively
u, w	velocity components along the radial and axial directions respectively
η	similarity parameter
ρ	density
μ	viscosity
υ	kinematic viscosity
ψ	stream function
σ_e	electrical conductivity
μ_m	magnetic permeability

TABLE 1. Dimensionless axial velocity $f(\eta)$ on three grid levels and their extrapolated values for $A = 1.2$, $R = -20$ and $M = 0.4$.

η	$f(\eta)$			
	$h = 0.02$	$h = 0.01$	$h = 0.005$	Extrapolated Value
-1.0	-0.2	-0.2	-0.2	-0.2
-0.8	-0.13873	-0.13874	-0.13874	-0.13874
-0.6	0.015705	0.015685	0.015674	0.01567
-0.4	0.212566	0.21253	0.212511	0.212503
-0.2	0.408992	0.408947	0.408922	0.408912
0	0.583823	0.583778	0.58375	0.58374
0.2	0.730454	0.730412	0.730383	0.730372
0.4	0.846692	0.846653	0.846624	0.846612
0.6	0.931164	0.931128	0.931098	0.931086
0.8	0.982675	0.98264	0.982609	0.982597
1.0	1.000092	1.000058	1.000028	1.000016

TABLE 2. Shear stresses at the disks for $R = -10$, $M = 0.8$ and various values of A.

A	$f''(-1)$	$f''(1)$	k
1.0	3.2842	0.9289	-9.8545
1.2	3.0954	1.1821	-12.5405
1.4	2.8918	1.4726	-15.6245
1.6	2.7342	1.8042	-19.1472
1.8	2.6378	2.1781	-23.1204
2.0	2.5936	2.5936	-23.1204

TABLE 3. Shear stresses at the disks for $A = 1.4$, $M = 1.2$ and various values of R.

R	$f''(-1)$	$-f''(1)$	k
0	2.1000	2.1000	-2.10005
-5	2.9464	1.9067	-11.817
-10	3.3323	1.8899	-21.3358
-15	3.5665	1.8839	-30.7645
-40	4.0636	1.8723	-77.505
-65	4.2439	1.8680	-124.062
-90	4.3381	1.8657	-170.57

TABLE 4. Shear stresses at the disks for $A = 1.2$, $R = -20$ and various values of M.

M	$f''(-1)$	$-f''(1)$	k
0.0	3.3069	0.7999	-15.998
0.4	3.3722	0.8802	-17.7447
0.8	3.6297	1.1245	-23.19
1.2	4.1361	1.5297	-32.664
1.6	4.8451	2.0753	-46.288
2.0	5.6813	2.7322	-64.012
2.4	6.5921	3.4736	-85.755
3.2	8.5312	5.1317	-141.075
4.0	10.5475	6.9396	-211.98
6.0	15.6995	11.7792	-456.876
8.0	20.8730	16.8030	-798.01

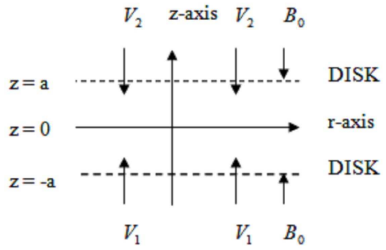

FIGURE 1. Geometry of the disks

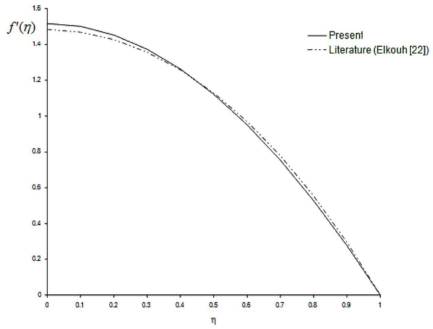

FIGURE 2. Comparison of the present dimensionless radial velocity profile with literature results (Elkouh [22]**) for** $R = -0.5$ **and** $M = 0$**.**

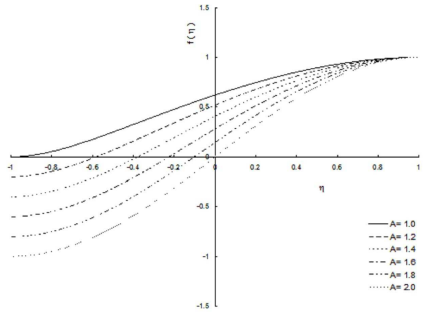

FIGURE 3. Variation of dimensionless axial velocity for $R = -10$**,** $M = 0.8$ **and various values of** A

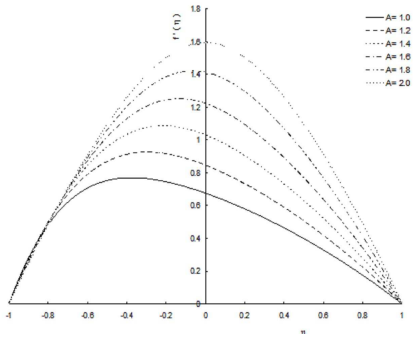

FIGURE 4. Variation of dimensionless radial velocity for $R = -10$, $M = 0.8$ and various values of A

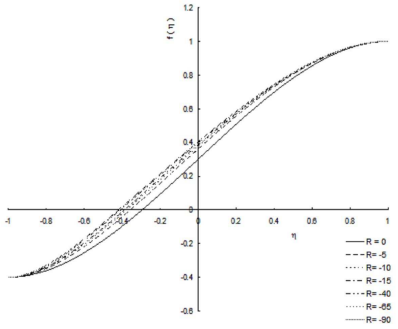

FIGURE 5. Variation of dimensionless axial velocity for $A = 1.4$, $M = 1.2$ and various values of R

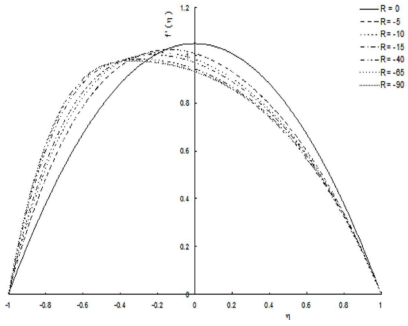

FIGURE 6. Variation of dimensionless radial velocity for $A = 1.4$, $M = 1.2$ and various values of R

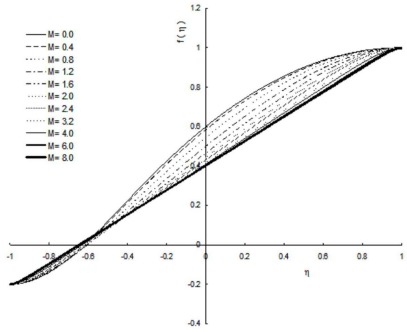

FIGURE 7. Variation of dimensionless axial velocity for $A = 1.2$, $R = -20$ and various values of M

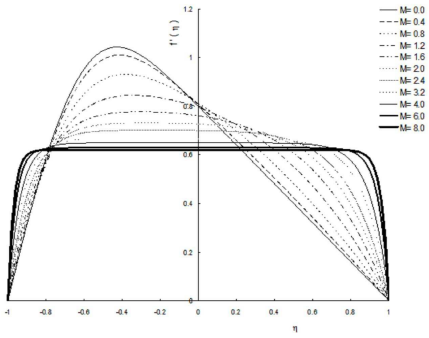

FIGURE 8. Variation of dimensionless radial velocity for $A = 1.2$, $R = -20$ and various values of M